Available online at www.sciencedirect.com
SCIENCE DIRECT®
International Journal of Heat and Fluid Flow 26 (2005) 587–596
International Journal of HEAT AND FLUID FLOW
www.elsevier.com/locate/ijhff

Natural convection in a rectangular enclosure with two heated sections on the lower surface

Patrick H. Oosthuizen *, Jane T. Paul

Department of Mechanical Engineering, Queen's University, Kingston, Ont., Canada K7L 3N6

Accepted 13 March 2005
Available online 31 May 2005

Abstract

The development of unsteady free convective flow in a rectangular enclosure has been numerically studied. The enclosure considered has rectangular horizontal lower and upper surfaces and vertical side surfaces. The horizontal width of enclosure is twice the vertical height and longitudinal length of the enclosure. There are two square isothermal heated sections on the lower surface, the rest of this surface being adiabatic. The vertical side-walls of the enclosure are kept at a uniform low temperature. The horizontal rectangular upper surface of the enclosure is either (a) adiabatic or (b) isothermal and at the same low temperature as the vertical side-walls. The governing unsteady, three-dimensional flow equations, written in dimensionless form, have been solved using an iterative, semi-implicit finite-difference method. The solution has the following parameters: the Rayleigh number, Ra, the Prandtl number, Pr, the dimensionless size, w_H, of the square heated sections and the dimensionless distance between the heated sections on the lower surface, w_S. Results have been obtained for a Prandtl number of 0.7. Most of the results presented here are for $w_H = w_S = 1/3$. The results indicate that for the flow situation considered the flow is steady at low Rayleigh numbers, becomes unsteady at intermediate Rayleigh numbers and then again becomes steady at higher Rayleigh numbers The conditions under which unsteady flow develops and the nature of the unsteady flow have been investigated and the variation of mean Nusselt number with Rayleigh number has been explored.

Keywords: Natural convection; Free convection; Unsteady flow; Enclosures; Numerical

1. Introduction

In a number of practically important situations involving natural convective flow in an enclosure, the flow becomes unsteady and three-dimensional at relatively low Rayleigh numbers. In order to study the development of such unsteady flows in relatively complex situations, flow in a rectangular enclosure with two separate heated sections on the lower surface has been numerically studied. The enclosure considered has rectangular horizontal lower and upper surfaces and vertical side surfaces. There are two square, symmetrically placed isothermal heated sections on the lower surface, the rest of this surface being adiabatic. The vertical side-walls of the enclosure are kept at a uniform low temperature while the horizontal rectangular upper surface is either adiabatic or isothermal and at the same low temperature as the vertical side-walls. The flow situation considered is therefore as shown in Fig. 1 and the positioning of the heated sections on the lower surface of the enclosure is as shown in Fig. 2.

In the situation considered, a steady flow exist at low Rayleigh numbers, an unsteady flow develops at higher Rayleigh numbers but the flow then again becomes

* Corresponding author. Tel.: +1 613 533 2573; fax: +1 613 533 6489.
E-mail address: oosthuiz@me.queensu.ca (P.H. Oosthuizen).

0142-727X/$ - see front matter © 2005 Elsevier Inc. All rights reserved.
doi:10.1016/j.ijheatfluidflow.2005.03.006

Nomenclature

g	gravitational acceleration
k	thermal conductivity
Nu_H	spatially averaged hot section mean Nusselt number based on q'_{wm}, W' and $T'_C - T'_H$
$\overline{Nu}$	time and spatially averaged mean Nusselt number based on $\overline{q'_{wm}}$, W' and $T'_C - T'_H$
$\overline{Nu_m}$	mean Nusselt number averaged over heated sections
Pr	Prandtl number
q'_{wm}	spatially averaged instantaneous heat transfer rate
$\overline{q'_{wm}}$	spatially and time averaged heat transfer rate
Ra	Rayleigh number based on W' and on $T'_H - T'_C$
t'	time
t	dimensionless time
T'	temperature
T	dimensionless temperature
T'_C	temperature of cold walls
T'_H	temperature of hot sections on lower surface
u'	velocity component in x' direction
u	dimensionless velocity component in x direction
v'	velocity component in y' direction
v	dimensionless velocity component in y direction
W'	size of enclosure
w'	velocity component in z' direction
w	dimensionless velocity component in z direction
w'_H	size of heated wall section
w_H	dimensionless size of heated wall section, w'_H/W'
w'_S	distance between heated wall sections
w_S	dimensionless distance between heated wall section, w'_S/W'
x'	horizontal coordinate
x	dimensionless horizontal coordinate
y'	horizontal coordinate
y	dimensionless horizontal coordinate
z'	vertical coordinate
z	dimensionless vertical coordinate
Greeks	
α	thermal diffusivity
β	bulk coefficient
ΔNu	difference between maximum and minimum values of spatially averaged Nusselt numbers
Φ'_x	x' component of vector potential
Φ'_y	y' component of vector potential
Φ'_z	z' component of vector potential
Φ_x	dimensionless Φ'_x
Φ_y	dimensionless Φ'_y
Φ_z	dimensionless Φ'_z
Ψ'_x	x' component of vector potential
Ψ'_y	y' component of vector potential
Ψ'_z	z' component of vector potential
Ψ_x	dimensionless Ψ'_x
Ψ_y	dimensionless Ψ'_y
Ψ_z	dimensionless Ψ'_z
ν	kinematic viscosity

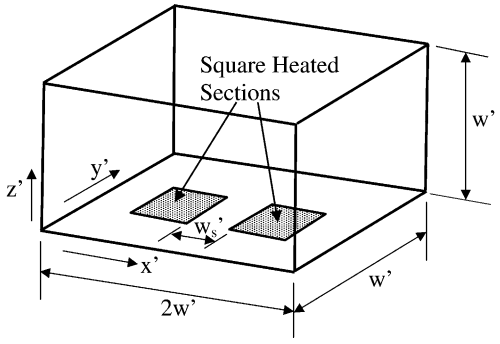

Fig. 1. Flow situation considered.

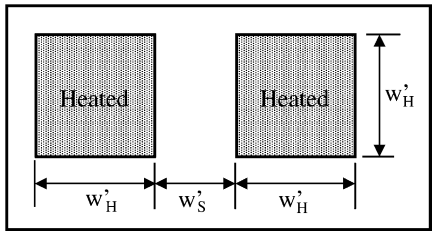

Fig. 2. Positioning of heated sections on lower surface of enclosure.

steady at still higher Rayleigh numbers. The flow situation considered is an approximate model of some electronic cooling situations. However, the main aim of the present study was basically to try to determine the conditions under which the unsteady flow develops and ceases and to examine some of the characteristics of the unsteady flow and to determine the effect of the flow unsteadiness on the mean heat transfer rate from the heated surfaces.

The flow situation being considered here, involving as it does a heated horizontal upward facing surfaces, is related to Rayleigh-Bénard convection. There have been a very large number of studies of Rayleigh-Bénard convection over, approximately, the past one hundred years,

reviews of some of these studies being given by Chandrasekhar (1981), Koschmieder (1993), Muller (1982), Tritton (1977) and Turner (1979). A large number of flow patterns, both two-dimensional and three-dimensional, are possible in Rayleigh-Bénard convection as discussed, for example, by Catton (1972), Davis (1967), Farhadieh and Tankin (1974) and Linthorst et al. (1981).

While classical Rayleigh-Bénard convection occurs between infinite parallel surfaces, the bottom being a high temperature and the top at a low temperature, similar flows occur in an enclosure with a heated lower surface and a cooled upper surface, e.g., see (Aziz and Hellums, 1967; Arroyo and Savirón, 1992; Catton, 1970, 1988; Gelfgat, 1999; Gollub and Benson, 1980; Heitz and Westwater, 1971; Hernández and Frederick, 1994; Huerta and Fernández-Mendez, 2001; Kirchartz and Oertel, 1988; Kolodner et al., 1986; Krishnamurti, 1981; Leong et al., 1998, 1999; Maveety, 1997; Mukutmoni and Yang, 1992; Oosthuizen, 1999, 2000, 2001a,b,c; Oosthuizen and Paul, 1998; Ozoe et al., 1976; Pallarès et al., 2001; Stellar et al., 1993; Stork and Muller, 1972; Tang and Tsang, 1997; Yang, 1988). When the lower surface is only partly heated complex flows related to those that occur in Rayleigh-Bénard convection also arise, e.g., see (Oosthuizen, 2002, 2003; Oosthuizen and Paul, 2002, 2003a,b,c; Sezai and Mohamad, 2000). In the situation being considered here where there are two separate heated sections on the lower surface there is the potential for complex flows resulting from the Rayleigh-Bénard type situation and due to the interaction of the flows rising from the separate heated sections on the lower surface.

2. Solution procedure

It has been assumed that the fluid properties are constant except for the density change with temperature which gives rise to the buoyancy forces, this having been treated by using the Boussinesq approach. The solution has been obtained by numerically solving the unsteady form of the governing equations.

The solution has been obtained in terms of the vorticity vector and vector potential functions which are defined by

$$u' = \frac{\partial \Psi'_z}{\partial y'} - \frac{\partial \Psi'_y}{\partial z'}, \quad v' = \frac{\partial \Psi'_x}{\partial z'} - \frac{\partial \Psi'_z}{\partial x'}, \quad w' = \frac{\partial \Psi'_y}{\partial x'} - \frac{\partial \Psi'_x}{\partial y'} \tag{1}$$

$$\Phi'_x = \frac{\partial w'}{\partial y'} - \frac{\partial v'}{\partial z'}, \quad \Phi'_y = \frac{\partial u'}{\partial z'} - \frac{\partial w'}{\partial x'}, \quad \Phi'_z = \frac{\partial v'}{\partial x'} - \frac{\partial u'}{\partial y'} \tag{2}$$

The coordinate system being used is shown in Fig. 1.

The following dimensionless variables have been introduced:

$$\begin{aligned} &\Phi_x = \Phi'_x/\alpha, \quad \Phi_y = \Phi'_y/\alpha, \quad \Phi_z = \Phi'_z/\alpha, \\ &\Psi_x = \Psi'_x W'^2/\alpha, \quad \Psi_y = \Psi'_y W'^2/\alpha, \quad \Psi_z = \Psi'_z W'^2/\alpha, \\ &u = u'W'/\alpha, \quad v = v'W'/\alpha, \quad w = w'W'/\alpha, \\ &T = (T' - T'_C)/(T'_H - T'_C), \quad t = t'\nu/W'^2 \end{aligned} \tag{3}$$

In terms of these dimensionless variables the governing equations are:

$$\Phi_x = -\left(\frac{\partial^2 \Psi_x}{\partial x^2} + \frac{\partial^2 \Psi_x}{\partial y^2} + \frac{\partial^2 \Psi_x}{\partial z^2}\right) \tag{4}$$

$$\Phi_y = -\left(\frac{\partial^2 \Psi_y}{\partial x^2} + \frac{\partial^2 \Psi_y}{\partial y^2} + \frac{\partial^2 \Psi_y}{\partial z^2}\right) \tag{5}$$

$$\Phi_z = -\left(\frac{\partial^2 \Psi_z}{\partial x^2} + \frac{\partial^2 \Psi_z}{\partial y^2} + \frac{\partial^2 \Psi_z}{\partial z^2}\right) \tag{6}$$

$$\begin{aligned} &Pr\frac{\partial \Phi_x}{\partial t} + \frac{\partial v\Phi_x}{\partial y} + \frac{\partial v\Phi_x}{\partial z} - \frac{\partial u\Phi_y}{\partial y} - \frac{\partial u\Phi_z}{\partial z} \\ &\quad = Pr\left(\frac{\partial^2 \Phi_x}{\partial x^2} + \frac{\partial^2 \Phi_x}{\partial y^2} + \frac{\partial^2 \Phi_x}{\partial z^2}\right) + RaPr\frac{\partial T}{\partial y} \end{aligned} \tag{7}$$

$$\begin{aligned} &Pr\frac{\partial \Phi_y}{\partial t} + \frac{\partial u\Phi_y}{\partial x} + \frac{\partial w\Phi_y}{\partial z} - \frac{\partial v\Phi_x}{\partial x} - \frac{\partial v\Phi_z}{\partial z} \\ &\quad = Pr\left(\frac{\partial^2 \Phi_y}{\partial x^2} + \frac{\partial^2 \Phi_y}{\partial y^2} + \frac{\partial^2 \Phi_y}{\partial z^2}\right) + RaPr\frac{\partial T}{\partial x} \end{aligned} \tag{8}$$

$$\begin{aligned} &Pr\frac{\partial \Phi_z}{\partial t} + \frac{\partial u\Phi_z}{\partial x} + \frac{\partial v\Phi_z}{\partial y} - \frac{\partial w\Phi_x}{\partial x} - \frac{\partial w\Phi_y}{\partial y} \\ &\quad = Pr\left(\frac{\partial^2 \Phi_z}{\partial x^2} + \frac{\partial^2 \Phi_z}{\partial y^2} + \frac{\partial^2 \Phi_z}{\partial z^2}\right) \end{aligned} \tag{9}$$

$$Pr\frac{\partial T}{\partial t} + \frac{\partial uT}{\partial x} + \frac{\partial vT}{\partial y} + \frac{\partial wT}{\partial z} = \left(\frac{\partial^2 T}{\partial x^2} + \frac{\partial^2 T}{\partial y^2} + \frac{\partial^2 T}{\partial z^2}\right) \tag{10}$$

$$u = \frac{\partial \Psi_z}{\partial y} - \frac{\partial \Psi_y}{\partial z}, \quad v = \frac{\partial \Psi_x}{\partial z} - \frac{\partial \Psi_z}{\partial x}, \quad w = \frac{\partial \Psi_y}{\partial x} - \frac{\partial \Psi_x}{\partial y} \tag{11}$$

Here, Ra is the Rayleigh number given by

$$Ra = \frac{\beta g (T'_H - T'_C) W'^3}{\nu\alpha} \tag{12}$$

The dimensionless velocity components u, v and w could have been eliminated between these equations. They have, however, been retained for numerical convenience.

The boundary conditions on these equations are that all velocity components are zero on all solid walls, that the dimensionless temperature is 1 on the heated portion of the lower horizontal surface, that the temperature gradients normal to all the remaining unheated portions of the lower surface are zero, that the dimensionless temperature is 0 on the vertical side surfaces, and on the horizontal upper surface either the temperature gradients normal to the wall surface are zero (adiabatic surface) or the dimensionless temperature is 0 (isothermal surface).

The dimensionless equations discussed above were solved using an iterative, semi-implicit finite-difference

method. The initial conditions were assumed to be that the velocity is everywhere zero and that the dimensionless temperature is everywhere equal 0.5. The solution was continued in dimensionless time until the time-averaged values of the flow variables ceased to change with time. Extensive grid- and time-step independence testing was undertaken involving changing the number of grid points in stages by 75% and the dimensionless time step in stages by 100%. In higher Rayleigh number cases where unsteady flow did not develop, the maximum dimensionless time to which the solution was continued was increased by up 100% to ensure that unsteady flow did not in fact occur at larger dimensionless times.

The solution for the temperature distribution allows the local dimensionless heat transfer rates over the heated and cooled surfaces to be determined. This distribution can then be spatially integrated over the surface at a given time to give the instantaneous spatially averaged dimensionless heat transfer rate, which is expressed in the form of a spatially averaged instantaneous Nusselt number:

$$Nu = \frac{q'_{wm} W'}{k(T'_{\mathrm{H}} - T'_{\mathrm{C}})} \tag{13}$$

q'_{wm} being the spatially averaged instantaneous heat transfer rate. These spatially averaged values of the dimensionless heat transfer rate can then be integrated in time to give the time and spatially averaged mean heat transfer rate, this being expressed in terms of the time and spatially averaged mean Nusselt number

$$\overline{Nu} = \frac{\overline{q'_{wm}} W'}{k(T'_{\mathrm{H}} - T'_{\mathrm{C}})} \tag{14}$$

$\overline{q'_{wm}}$ being the spatially and time averaged heat transfer rate.

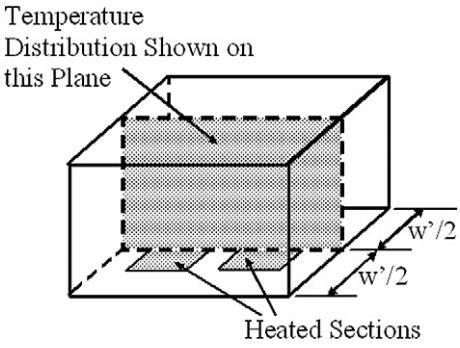

Fig. 4. Vertical centre-plane on which temperature distribution is shown.

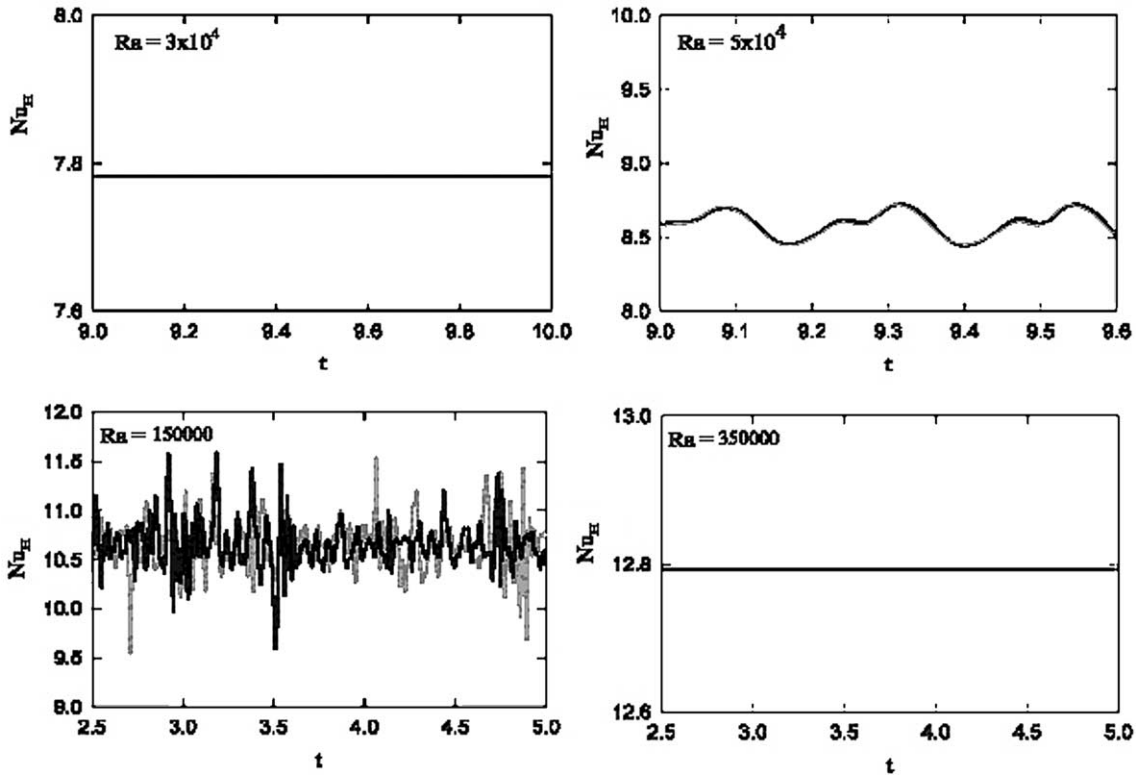

Fig. 3. Variation of spatially averaged Nusselt number for hot surfaces with dimensionless time for Rayleigh numbers of 3×10^4 (top left), 5×10^4 (top right), 1.5×10^5 (bottom left) and 3.5×10^5 (bottom right) for adiabatic upper surface case for $w_{\mathrm{H}} = 1/3$ and $w_{\mathrm{S}} = 1/3$.

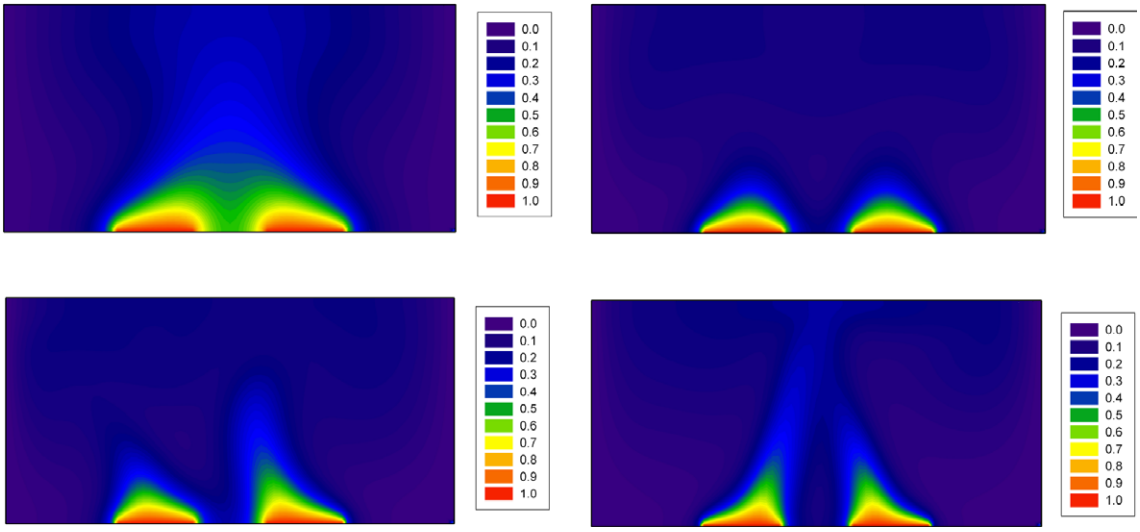

Fig. 5. Typical instantaneous dimensionless temperature variations over the vertical centre-plane of the enclosure for Rayleigh numbers of 10^4 (top left), 5×10^4 (top right), 8×10^4 (bottom left) and 2.35×10^5 (bottom right) for adiabatic upper surface case.

3. Results

The solution has the following parameters:

1. the Rayleigh number, *Ra*,
2. the Prandtl number, *Pr*,
3. the dimensionless size, w_H, of the square heated sections,
4. the dimensionless distance between the heated sections on the lower surface, w_S
5. the boundary condition on the upper surface, i.e., either adiabatic or isothermal.

Because of the applications that originally motivated this work (electronic cooling), results have only been obtained for a Prandtl number of 0.7. Results for a w_H value of 1/3 will be presented here, results obtained with other values of w_H showing the same basic characteristics as those presented here. Most of the results presented will be for a w_S value of 1/3, results for other values of w_S up to 1 displaying the same basic characteristics as those given here.

Results for the case where the horizontal upper surface of the enclosure is adiabatic will first be considered and results for a w_S value of 1/3 and a w_H value of 1/3 will first be discussed. As previously mentioned, a steady flow exists at low Rayleigh numbers but the flow becomes unsteady when the Rayleigh number exceeds a critical value. However the flow then again becomes

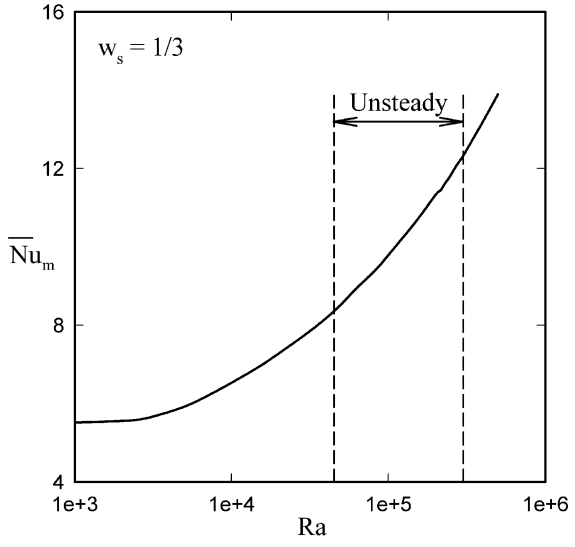

Fig. 6. Variation of mean Nusselt number with *Ra* for $w_H = 1/3$ and $w_S = 1/3$ for adiabatic upper surface case.

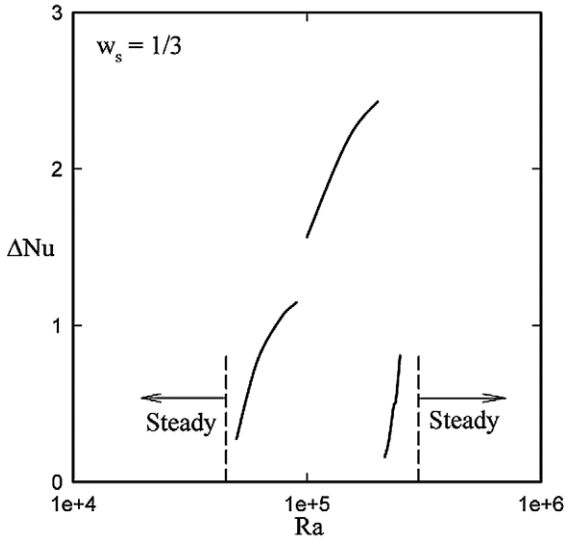

Fig. 7. Variation of Nusselt number difference with *Ra* for $w_H = 1/3$ and $w_S = 1/3$ for adiabatic upper surface case.

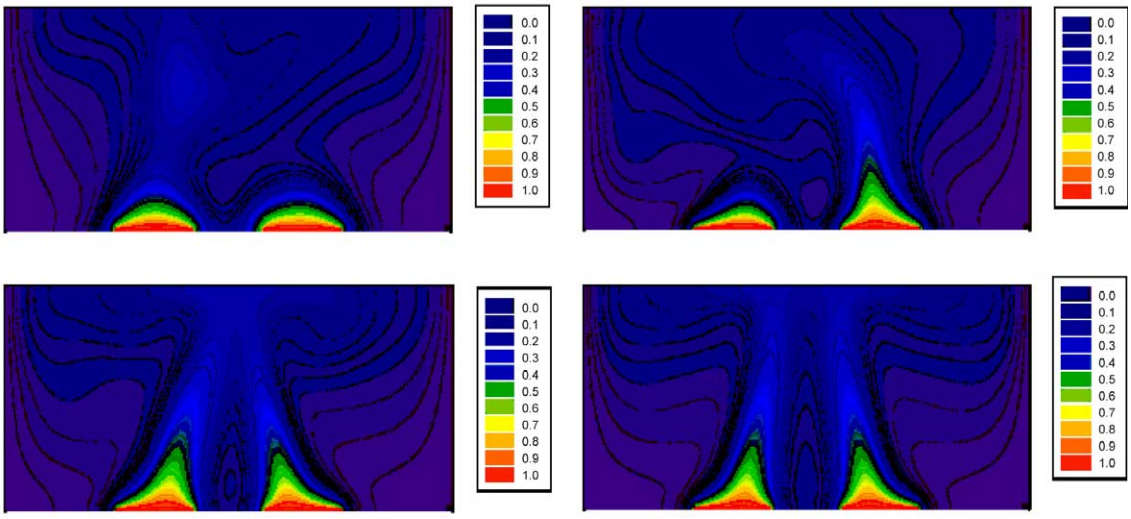

Fig. 8. Instantaneous dimensionless temperature variations over the vertical centre-plane of the enclosure for Rayleigh numbers of 6×10^4 (top left), 1.5×10^5 (top right), 2.4×10^5 (bottom left) and 2.75×10^5 (bottom right) for adiabatic upper surface case.

steady at higher Rayleigh numbers. The change from steady to unsteady flow and then back to steady flow can be illustrated by considering the variation of the instantaneous spatially averaged Nusselt number for the hot surface, *Nu*, with dimensionless time for various values of *Ra*. Typical such variations are shown in Fig. 3. The flow will be seen to change from steady to periodic and then to more complex flows and then back to steady as the Rayleigh number is increased. The reasons for the observed unsteady behavior can be partly deduced by considering the instantaneous isotherm patterns on the vertical centre-plane (i.e. on the x–z plane at $y = 0.5$ see Fig. 4) at various Rayleigh numbers. Typical such patterns are shown in Fig. 5. It will be seen that at low Rayleigh numbers the "plumes" rising from each heated section merge very near the lower surface and rise from this surface essentially as single "plume" (the term "plume" is used here to indicate the strong convective flow rising from the heated surfaces, this flow of course turning near the top surface and then descending along the cooled vertical walls of the enclosure). However at higher Rayleigh numbers the "plumes" above each surface interact but do not truly merge, the interaction leading to the observed unsteady flow. At still higher Rayleigh numbers, the "plumes" remain essentially independent of each other and the flow again becomes steady. Of course at even higher Rayleigh numbers instability will develop in each individual "plume" and the flow will again become unsteady.

The variation of the time and spatially averaged mean Nusselt numbers averaged for the two heated wall sections with Rayleigh number is shown in Fig. 6. It will be seen that there are no sharp jumps in the variation that could result from the development of unsteady flow and from the sharp changes that occur in the unsteady flow pattern.

The variation of the average (for the two heated surfaces) difference between the maximum and minimum values of the instantaneous spatially averaged Nusselt numbers with Rayleigh number is shown in Fig. 7. This average Nusselt number difference is defined by

$$\Delta Nu = \frac{1}{2}\left[(Nu_{\max} - Nu_{\min})_1 + (Nu_{\max} - Nu_{\min})_2\right]$$

the numbers 1 and 2 referring to the values for the two heated sections.

It will be seen from Fig. 7 that unsteady flow starts at a Rayleigh number of approximately 4.5×10^4 and that steady flow again occurs when the Rayleigh number exceeds a value of approximately 2.7×10^5. It will also be seen that there are sharp jumps in the variation. This

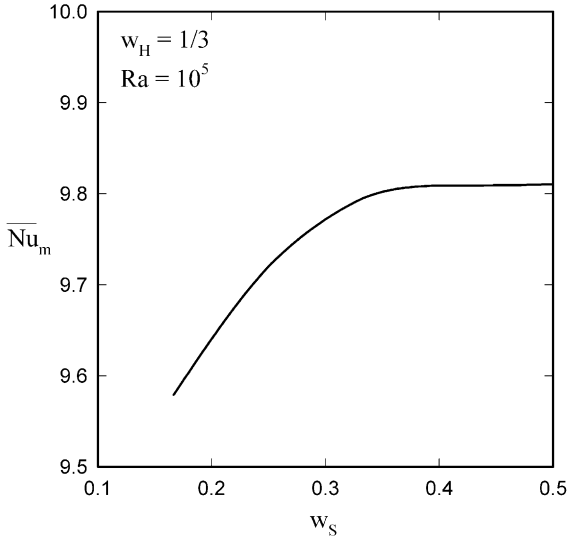

Fig. 9. Variation of mean Nusselt number with w_S for $w_H = 1/3$ and $Ra = 10^5$ for adiabatic upper surface case.

arises because of sharp changes in the unsteady flow pattern. These changes are illustrated by the centre-plane (see Fig. 4) isotherm patterns shown in Fig. 8. These isotherm patterns are for Rayleigh numbers near the middle of each of three curves segments shown in Fig. 7 and for a Rayleigh number above that at which the flow again becomes steady. At the lowest Rayleigh number considered in Fig. 8, the flow basically involves hot gas bursts rising alternatively from each heated section. At the second Rayleigh number considered, heated plumes rise alternatively from each of the heated sections. At the third Rayleigh number considered, heated plumes rise continuously from each heated section, these plumes interacting near the upper surface leading to the observed unsteady flow. At the highest Rayleigh number considered, heated plumes again rise continuously from each heated section, these plumes, while converging to some extent as a result of the induced inflow associated with the rising plumes, do not interact before reaching the upper surface and no unsteadiness develops in the flow field. The largest values of ΔNu occur in the middle range of Rayleigh numbers considered.

The effect of the dimensionless distance, w_S, between the two heated sections will lastly be considered. The effect of this dimensionless distance on the time and spatially averaged mean Nusselt number averaged for the two heated wall sections at a fixed Rayleigh number is shown in Fig. 9. It will be seen from Fig. 9 that the mean Nusselt number is essentially independent of w_S for w_S values above 0.3. For smaller values of w_S, the strong interaction between the flows from the two heated sections leads to a reduction in the heat transfer rate. Of course, for w_S values much larger than those considered here, the heat transfer rate becomes more strongly affected by the presence of the vertical walls of the enclosure.

The results discussed above were all for the case where the upper horizontal surface of the enclosure is adiabatic. Attention will next be turned to the case where this upper horizontal surface is isothermal, the dimensionless temperature on this surface being given by $T = 0$, the same value as exists on the vertical sidewalls of the enclosure. Results will only be presented here for the case where $w_H = w_S = 1/3$, results for other values of these parameters having the same basic form as those given here.

The results obtained for the isothermal upper surface case indicate that, as was the case when the upper surface was adiabatic, the flow in the enclosure is steady at the lower Rayleigh numbers but that when the

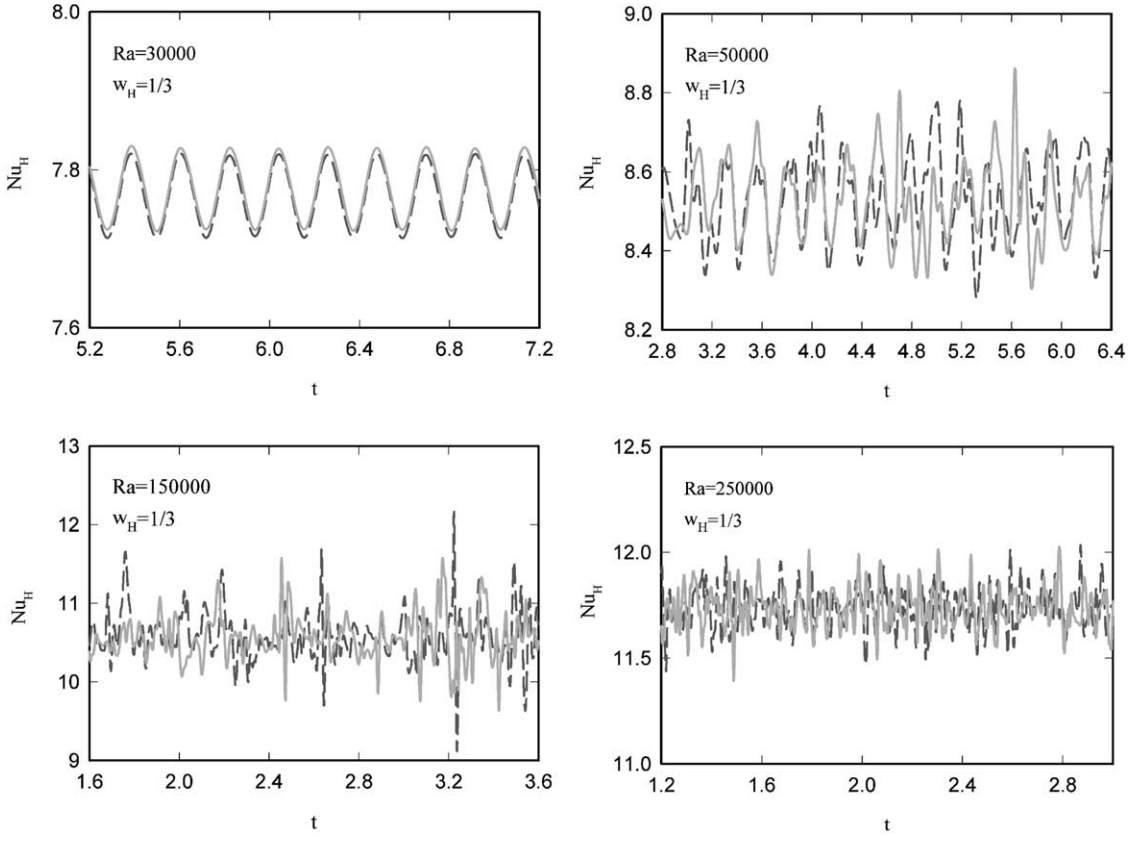

Fig. 10. Variation of spatially averaged Nusselt number for hot surfaces with dimensionless time for Rayleigh numbers of 3×10^4 (top), 5×10^4 (second from top), 1.5×10^5 (third from top) and 2.5×10^5 (bottom) for isothermal upper surface case for $w_H = 1/3$ and $w_S = 1/3$.

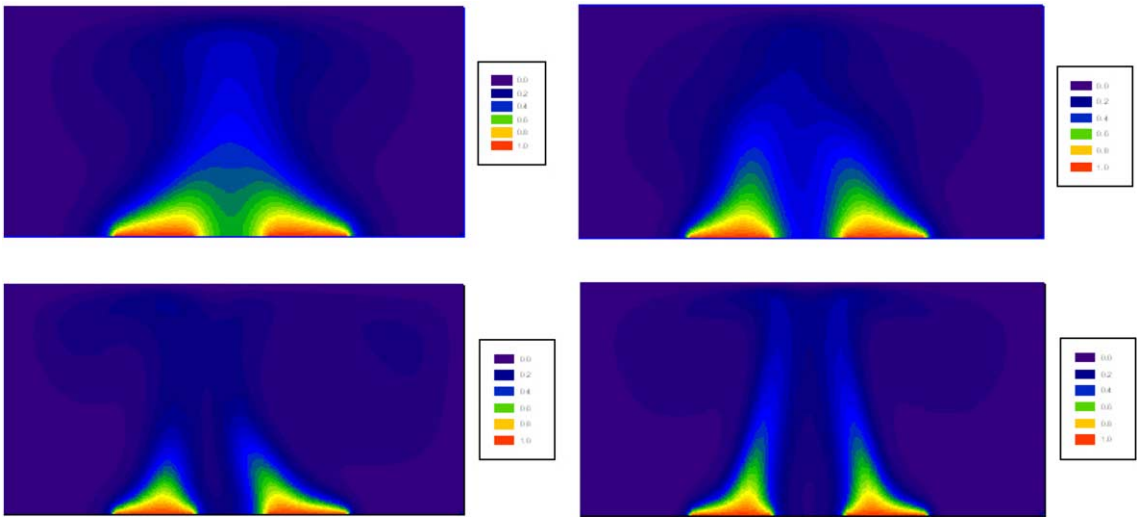

Fig. 11. Typical instantaneous dimensionless temperature variations over the vertical centre-plane of the enclosure for Rayleigh numbers of 2×10^4 (top), 10^5 (second from top), 2×10^5 (third from top) and 2.5×10^5 (bottom) for isothermal upper surface case for $w_H = 1/3$ and $w_S = 1/3$.

Rayleigh number exceeds a critical value the flow becomes unsteady, the flow then again becomes steady at higher Rayleigh numbers. This development of the unsteady flow is illustrated by the results given in Fig. 10 which show the typical variations of the instantaneous spatially averaged Nusselt numbers with dimensionless time for various Rayleigh number values. As with the adiabatic upper surface case, at the lowest Rayleigh number considered the flow varies in a relatively simple manner with time but at highest Rayleigh numbers considered the flow varies in a complex multi-periodic manner with time. Over a narrow range of Rayleigh numbers just above that at which the unsteady flow first occurs, the Nusselt number varies in a simple periodic manner with time, this being illustrated by the results given in Fig. 10.

As discussed for the adiabatic upper surface case, an idea of the nature of the flow in the enclosure can be gained by considering the instantaneous temperature distribution at a particular instant of time on the vertical centre-plane of the enclosure, this plane being shown in Fig. 4. Typical instantaneous centre-plane distributions for various Rayleigh numbers are shown in Fig. 11.

The variation of the time and spatially averaged mean Nusselt number averaged for the two heated wall sections with Rayleigh number for the isothermal upper surface case is shown in Fig. 12. A comparison of the results given in Fig. 12 for the isothermal upper wall case with those given in Fig. 6 for the adiabatic upper wall case shows that the biggest difference between the results for the two cases exists at the lower Rayleigh numbers. In the isothermal upper wall case the Nusselt number stays essentially at its conduction value up to a Rayleigh number of approximately 10^4 before it rises sharply to a value that is close to that which exits in the adiabatic upper surface case. The presence of the cold isothermal upper surface therefore tends to suppress the development of the convective motion in the enclosure at lower Rayleigh numbers. Another difference between the two sets of results is that the unsteady flow starts at a Rayleigh number of approximately 4.5×10^4 and ends at a Rayleigh number of approximately 2.7×10^5 in the adiabatic upper wall case whereas it starts at a value of approximately 2.6×10^4 and ends at a value of approximately 3×10^5 in the isothermal upper surface case. However, while the values for the two cases are different, the differences will be seen to be relatively small.

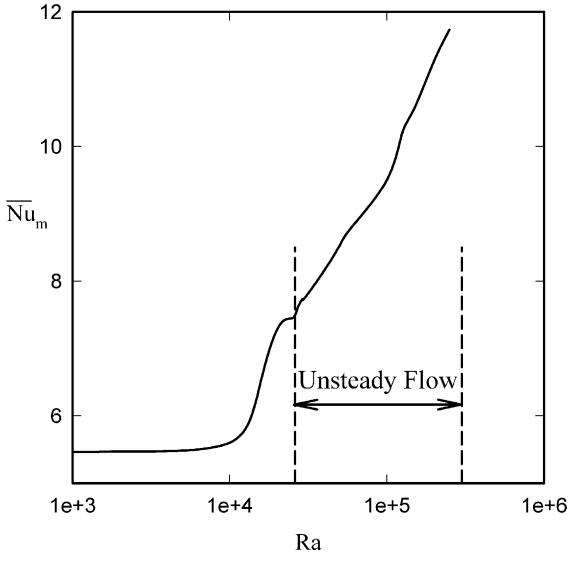

Fig. 12. Variation of mean Nusselt number with w_S for $w_H = 1/3$ and $Ra = 10^5$ for isothermal upper surface case.

4. Conclusions

The results of the present study indicate that:

1. For the flow situation considered here the flow is steady at low Rayleigh numbers, becomes unsteady at intermediate Rayleigh numbers and then again becomes steady at higher Rayleigh numbers. The unsteadiness that develops results from the interaction of the flows rising from each of the heated sections.
2. Sharp changes in the nature of the unsteady flow pattern occur with changes in Rayleigh number.
3. Despite the sharp changes in the flow pattern that occur with changes in Rayleigh number in the unsteady flow region, the variation of the mean Nusselt number with Rayleigh number is essentially smooth.
4. The upper surface thermal boundary condition (adiabatic or isothermal) does not have a strong effect on the basic characteristics of the enclosure flow.
5. When considering the mean Nusselt number variation with Rayleigh number, the largest effect of the upper surface boundary condition occurs at relatively low Rayleigh numbers.

Acknowledgement

This work was supported by the Natural Sciences and Engineering Research Council of Canada.

References

Aziz, K., Hellums, J.D., 1967. Numerical solution for the three-dimensional equations of motion for laminar natural convection. Phys. Fluids 10 (2), 314–324.

Arroyo, M.P., Savirón, J.M., 1992. Rayleigh Bénard convection in a small box: spatial features and thermal dependence of the velocity field. J. Fluid Mech. 235, 325–348.

Catton, I., 1970. Convection in a closed rectangular region: the onset of motion. J. Heat Transfer 92, 186–188.

Catton, I., 1972. The effect of insulating vertical walls on the onset of motion in a fluid heated from below. Int. J. Heat Mass Transfer 15, 665–672.

Catton, I., 1988. Wavenumber selection in Bénard convection. J. Heat Transfer 110, 1154–1165.

Chandrasekhar, S., 1981. Hydrodynamic and Hydromagnetic Stability. Dover, New York.

Davis, S.H., 1967. Convection in a box: linear theory. J. Fluid Mech. 30, 465–478.

Farhadieh, R., Tankin, R.S., 1974. Interferometric study of two-dimensional Bénard convection cells. J. Fluid Mech. 66, 739–752.

Gelfgat, A.Y., 1999. Different modes of Rayleigh Bénard instability in two- and three-dimensional rectangular enclosures. J. Comput. Phys. 156, 300–324.

Gollub, J.P., Benson, S.V., 1980. Many routes to turbulent convection. J. Fluid Mech. 100, 449–470.

Heitz, W.L., Westwater, J.W., 1971. Critical Rayleigh numbers for natural convection of water confined in square cells with L/D from 0.5 to 8. J. Heat Transfer 93, 188–196.

Hernández, H., Frederick, R.L., 1994. Spatial and thermal features of three-dimensional Rayleigh-Bénard convection. Int. J. Heat and Mass Transfer 37 (3), 411–424.

Huerta, A., Fernández-Mendez, S., 2001. Time accurate consistently stabilized mesh-free methods for convection dominated problems. Int. J. Numer. Methods Eng. 50, 1–18.

Kirchartz, K.R., Oertel, H., 1988. Three-dimensional thermal cellular convection in rectangular boxes. J. Fluid Mech. 192, 249–286.

Kolodner, P., Walden, R.W., Passner, A., Surko, C.M., 1986. Rayleigh-Bénard convection in an intermediate-aspect-ratio rectangular container. J. Fluid Mech. 163, 195–226.

Koschmieder, E.L., 1993. Bénard Cells and Taylor Vortices. Cambridge University Press, Cambridge.

Krishnamurti, R., 1981. Generation of large scale circulation in turbulent convection. Proc. Indian Acad. Sci.—Eng. Sci. Ser. 4 (3), 277–293.

Leong, W.H., Hollands, K.G.T., Burnger, A.P., 1998. On a physically realizable benchmark problem in internal natural convection. Int. J. Heat Mass Transfer 41, 3817–3828.

Leong, W.H., Hollands, K.G.T., Burnger, A.P., 1999. Experimental Nusselt numbers for a cubical-cavity benchmark problem in natural convection. Int. J. Heat Mass Transfer 42, 1979–1989.

Linthorst, S.J.M., Schinkel, W.M.M., Hoogendoorn, C.J., 1981. Flow structure with natural convection in inclined air-filled enclosures. J. Heat Transfer 103, 535–539.

Maveety, J.G., 1997. Heat transfer in Rayleigh Bénard convection with air in moderate size containers. Int. J. Heat Mass Transfer 41 (4–5), 785–796.

Mukutmoni, D., Yang, K.T., 1992. Wavenumber selection for Rayleigh-Bénard convection in a small aspect ratio box. Int. J. Heat Mass Transfer 33, 2145–2159.

Muller, U., 1982. Bénard convection in gaps and cavities. In: Zierep, J., Oertel, H. (Eds.), Convective Transport and Instability. G. Braun, Karlsruhe, pp. 71–100.

Oosthuizen, P.H., 1999. A numerical study of three-dimensional natural convection in a low aspect ratio horizontal enclosure with a uniform heat flux on the lower surface. In: Proc. ASME Int. Mech. Eng. Congress and Exhibition (IMECE), HTD-vol. 364-1, pp. 145–152.

Oosthuizen, P.H., 2000. A numerical study of three-dimensional natural convection in an enclosure with a uniform heat flux on one vertical wall. In: Proc. ASME 2000 National Heat Transfer Conference.

Oosthuizen, P.H., 2001a. Effect of aspect ratio on three-dimensional natural convection in a horizontal enclosure with a uniform heat flux on the lower surface. In: Proc. 2nd Int. Workshop on Scientific Computing and ApplicationsAdvances in Computation: Theory and Practice, vol. 7. Nova Science Pub. Inc., pp. 237–246.

Oosthuizen, P.H., 2001b. A numerical study of the effect of aspect ratio on three dimensional natural convection in a horizontal enclosure with a uniform heat flux on the lower surface. In: Bilgen, E., Atagunduz, G., (Eds.), Proc. 4th Int. Thermal Energy Congress, 384–389.

Oosthuizen, P.H., 2001c. A numerical study of the development of unsteady three-dimensional natural convective flow in a horizontal enclosure with a uniform heat flux on the lower surface. In: Proc. 2001 ASME Int. Mech. Eng. Congress and Exposition (IMECE) Paper No. IMECE2001/HTD-24121.

Oosthuizen, P.H., 2002. Three-dimensional, unsteady natural convection in a partially heated horizontal enclosure. In: Proc. 8th AIAA/ASME Joint Thermophysics and Heat Transfer Conference, Paper AIAA 2002–3317.

Oosthuizen, P.H., 2003. Convection in a cubical enclosure with a partially heated lower surface and cooled side and top walls. In:

Mohamad, A.A. (Eds.), Proc. 3rd International Conference on Computational Heat and Mass Transfer (ICCHMT), pp. 638–646.

Oosthuizen, P.H., Paul, J.T., 2002. The development of three-dimensional, unsteady natural convection in a horizontal enclosure with a partially heated lower surface and cooled vertical side walls. In: Proc. 12th International Heat Transfer Conference, vol. 2, pp. 63–68.

Oosthuizen, P.H., Paul, J.T., 1998. A numerical study of three-dimensional natural convection in a horizontal enclosure with a uniform heat flux on the lower surface. In: Proc. 11th International Heat Transfer Conference, vol. 3, pp. 391–396.

Oosthuizen, P.H., Paul, J.T., 2003a. Effect of vertical aspect ratio on three-dimensional unsteady natural convection in a horizontal enclosure with a partially heated lower surface and cooled vertical side-walls. In: Proc. 6th ASME-JSME Thermal Engineering Joint Conference.

Oosthuizen, P.H., Paul, J.T., 2003b. Three-dimensional, unsteady natural convection in a horizontal enclosure with a heated strip on the lower surface and cooled side and top surfaces. In: Proc. 19th Canadian Congress of Applied Mechanics, vol. 2, pp. 220–221.

Oosthuizen, P.H., Paul, J.T., 2003c. Effect of vertical aspect ratio on three-dimensional, unsteady natural convection in a horizontal enclosure with a partially heated lower surface and cooled vertical side walls. In: Proc. 2nd International Conference on Heat Transfer, Fluid Mechanics and Thermodynamics (HEFAT).

Ozoe, H., Yamamoto, K., Churchill, K.S.W., Sayama, H., 1976. Three-dimensional, numerical analysis of laminar natural convection in a confined fluid heated from below. J. Heat Transfer 98, 202–207.

Pallarès, J., Arroya, M.P., Grau, F.X., Giralt, F., 2001. Experimental laminar Rayleigh-Bénard convection in a cubical cavity at moderate Rayleigh and Prandtl numbers. Exp. Fluids 31, 208–218.

Sezai, I., Mohamad, A.A., 2000. Natural convection from a discrete heat source on the bottom of a horizontal enclosure. Int. J. Heat Mass Transfer 43–13, 2257–2266.

Stellar, F., Guj, G., Leonardi, E., 1993. The Rayleigh-Bénard problem in intermediate bounded domains. J. Fluid Mech. 254, 375–400.

Stork, K., Muller, U., 1972. Convection in a box: experiments. J. Fluid Mech. 54, 599–611.

Tang, L.Q., Tsang, T.T.H., 1997. Temporal, spatial and thermal features of 3-D Rayleigh-Bénard convection by a least-squares finite element method. Comput. Methods Appl. Mech. Eng. 140, 201–219.

Tritton, D.J, 1977. Physical Fluid Dynamics. Van Nostrand Reinhold (UK) Co. Ltd., Wokingham, Berkshire, England, pp. 30–41.

Turner, J.S., 1979. Buoyancy Effects in Fluids. Cambridge University Press, Cambridge.

Yang, K.Y., Transitions and bifurcations in laminar buoyant flows in confined enclosures, J., 1988. Heat Transfer 110, 1191–1204.